

**TRANSIENT ANALYSIS OF LAMINATED  
COMPOSITE PLATES USING NURBS-BASED FINITE ELEMENTS**  
**PHÂN TÍCH ĐÁP ỨNG CỦA TẤM COMPOSITE NHIỀU LỚP SỬ DỤNG  
PHƯƠNG PHÁP PHẦN TỬ HỮU HẠN DỰA TRÊN HÀM NURBS**

**Nguyen Thi Bich Lieu<sup>1</sup>, Thai Hoang Chien<sup>2</sup>,  
Dang Thien Ngon<sup>1</sup>, Nguyen Xuan Hung<sup>3</sup>**

<sup>1</sup> Ho Chi Minh City University of Technology and Education

<sup>2</sup> Ho Chi Minh City Ton Duc Thang University

<sup>3</sup> Ho Chi Minh City University of Science, VNU-HCMC

**TÓM TẮT**

*Phân tích đẳng hình học (IGA), sự tích hợp giữa thiết kế và phân tích, được tìm thấy cho đến nay là các công cụ hiệu quả cho việc phân tích số của một loạt các bài toán thực tế. Bài báo này tiếp tục mở rộng phương pháp phần tử hữu hạn dựa trên hàm NURBS cho phân tích đáp ứng của tấm composite nhiều lớp bằng cách sử dụng lý thuyết biến dạng cắt bậc cao. Lý thuyết đưa ra được suy ra từ lý thuyết tấm cổ điển (CPT) và ứng suất cắt trên bề mặt tấm thỏa mãn điều kiện một cách tự nhiên. Vì vậy, không bắt buộc yếu tố hiệu chỉnh cắt. Dạng yếu Galerkin của mô hình phân tích đáp ứng tấm composite nhiều lớp được sử dụng để đạt được hệ thống các phương trình rời rạc. Nó có thể được giải quyết bằng phương pháp phân tích đẳng hình học dựa trên hàm NURBS. Một số ví dụ số của các tấm composite nhiều lớp dưới các tải trọng động khác nhau, các hướng sợi và nhiều lớp được đưa ra. Độ chính xác và độ tin cậy của phương pháp đề xuất được chứng minh bằng cách so sánh với các lời giải giải tích, lời giải số và phần mềm Ansys.*

**ABSTRACT**

*The isogeometric analysis (IGA) that integrates Computer Aided Design (CAD) and Computer Aided Engineering (CAE) is found so far the effectively numerical tool for the analysis of a variety of practical problems. This paper is further extended NURBS-based isogeometric approach for response analysis of laminated composite plates using the higher-order shear deformation theory. The present theory is derived from the classical plate theory (CPT) and the shear stress free surface conditions are naturally satisfied. Therefore, shear correction factors are not required. Galerkin weak form of response analysis model for laminated composite plate is used to obtain the discrete system of equations. It can be solved by NURBS-based isogeometric analysis. Some numerical examples of the laminated composite plates under various dynamic loads, fiber orientations and lay-up numbers are presented. The accuracy and reliability of the proposed method is verified by comparing with analytical, numerical solutions and Ansys software.*

**Keywords:** *Transient analysis, laminated composite plate, isogeometric analysis, NURBS, Newmark integration.*

**I. INTRODUCTION**

The transient response of laminated composite plates has received much attention from designers due to increasing applications

of composite in high performance aircraft, vehicles and vessels. Whether they are used in civil, marine or aerospace, most structures are subjected to dynamic loads during their

operation. Therefore, there exists a need for assessing the natural frequency and transient response of structures.

Many numerical methods have been developed to compute, analyze and simulate the response as well as dynamic characteristics of laminated composite plates. Out of these methods, the finite element method (FEM) has become the universally applicable technique for solving boundary and initial value problems. In the past years, Reismann [1], Reismann and Lee [2] have analyzed simply supported rectangular isotropic plates, which are subjected to suddenly a uniformly distributed load over a square area on the plate. The transient finite element analysis of isotropic plate was also carried out by Rock and Hinton [3] for thick and thin plates. Akay [4] determined the large deflection transient response of isotropic plates using a mixed FEM. For composite plates, Reddy [5] presented finite element results for the transient analysis of layered composite plates based on the first-order shear deformation theory (FSDT). Mallikarjuna and Kant [6] presented an isoparametric finite element formulation based on a higher-order displacement model for dynamic analysis of multi-layer symmetric composite plate. Wang and his co-workers developed the strip element method (SEM) for static bending analysis of orthotropic plates. Then, Wang extended the SEM to transient analysis of symmetric laminated plates [7].

Although FEM is an extremely versatile and powerful technique, it has certain disadvantages. Recently, Hughes and his co-workers have proposed a robustly computational isogeometric analysis (IGA) [8], which aims to unify the computer aided design (CAD) and the computer aided engineering (CAE) to benefit from the geometrical exactness operation in engineering problems. Following this approach, the CAD-shape functions, commonly the non-uniform rational B-splines (NURBS) are substituted for the Lagrange polynomial based shape

functions in the CAE. The computational cost is decreased significantly as the meshes are generated within the CAD. IGA gives higher accurate results because of the smoothness and the higher order continuity between elements [9,10].

In this paper, a higher order displacement fields in which the in plane displacement expressed as cubic functions of the thickness coordinate is presented. The finite element formulation based on the HSDT requires elements with at least  $C^1$ -inter-element continuity. It is difficult to achieve such elements for free-form geometries when using the standard Lagrangian polynomials as basic functions. However, in IGA can be easily obtained because NURBS basis functions are  $C^{p-1}$  continuous. The governing equations of the laminated composite plate are transformed into a standard weak-form, which is then discretized into an isogeometric system of time-dependent equations to be solved by the unconditionally stable Newmark time integration scheme. Several numerical examples with many different models are provided to illustrate the effectiveness and reliability of the present method in comparison with other results from the literature.

## II. THE HIGHER-ORDER SHEAR DEFORMATION THEORY FOR PLATES

Let  $\Omega$  be the domain in  $R^2$  occupied by the mid-plane of the plate and  $u_0, v_0, w$  and

$\beta = (b_x; b_y)^T$  denote the displacement components in the  $x; y; z$  directions and the rotations in the  $x-z$  and  $y-z$  planes (or the  $y$  and the  $x$  axes), respectively. Figure 1 shows the geometry of plate and coordinate system. A higher-order shear deformation theory derived from the classical plate theory is defined as follows [9]:

$$u(x, y, z, t) = u_0(x, y, t) - z \frac{\partial w(x, y, t)}{\partial x} + f(z) \beta_x(x, y, t)$$

$$\begin{aligned} v(x, y, z, t) &= v_0(x, y, t) - z \frac{\partial w(x, y, t)}{\partial y} + \\ & f(z) \beta_y(x, y, t) \\ w(x, y, z, t) &= w(x, y, t) \end{aligned} \quad (1)$$

In this paper, the third-order shear deformation theory (TSDT) of Reddy [11] is used and the distributed function is written as

$$f(z) = z - 4z^3 / 3h^2.$$

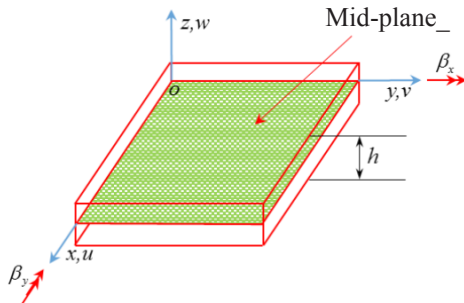


Figure 1. Plate model and coordinate system.

The relationship between strains and displacements is described by,

$$\boldsymbol{\varepsilon}_p = [\varepsilon_{xx} \ \varepsilon_{yy} \ \gamma_{xy}]^T = \boldsymbol{\varepsilon}_0 + z\boldsymbol{\varepsilon}_1 + f(z)\boldsymbol{\varepsilon}_2 \quad (2)$$

where

$$\boldsymbol{\gamma} = [\gamma_{xz} \ \gamma_{yz}]^T = f'(z)\boldsymbol{\varepsilon}_s$$

$$\begin{aligned} \boldsymbol{\varepsilon}_0 &= \begin{bmatrix} u_{0,x} \\ v_{0,y} \\ v_{0,x} + u_{0,y} \end{bmatrix}, \boldsymbol{\varepsilon}_1 = \begin{bmatrix} -w_{,xx} \\ -w_{,yy} \\ -2w_{,xy} \end{bmatrix}, \\ \boldsymbol{\varepsilon}_2 &= \begin{bmatrix} \beta_{x,x} \\ \beta_{y,y} \\ \beta_{y,x} + \beta_{x,y} \end{bmatrix}, \boldsymbol{\varepsilon}_s = \begin{bmatrix} \beta_x \\ \beta_y \end{bmatrix} \end{aligned} \quad (3)$$

Neglecting  $\sigma_z$  for each orthotropic layer, the constitutive equation of an orthotropic lamina in the local coordinate system is derived from Hooke's law for plane stress as

$$\begin{Bmatrix} \sigma_1^k \\ \sigma_2^k \\ \tau_{12}^k \\ \tau_{13}^k \\ \tau_{23}^k \end{Bmatrix} = \begin{bmatrix} Q_{11} & Q_{12} & 0 & 0 & 0 \\ Q_{12} & Q_{22} & 0 & 0 & 0 \\ 0 & 0 & Q_{33} & 0 & 0 \\ 0 & 0 & 0 & Q_{55} & 0 \\ 0 & 0 & 0 & 0 & Q_{44} \end{bmatrix}^k \begin{Bmatrix} \varepsilon_1^k \\ \varepsilon_2^k \\ \gamma_{12}^k \\ \gamma_{13}^k \\ \gamma_{23}^k \end{Bmatrix} \quad (4)$$

where subscripts 1 and 2 are the directions of the fiber and in-plane normal to fiber, respectively, subscript 3 indicates the direction normal to the plate; and the reduced stiffness

components,  $Q_{ij}^k$  are given by:

$$\begin{aligned} Q_{11}^k &= \frac{E_1^k}{1 - \nu_{12}^k \nu_{21}^k}; Q_{12}^k = \frac{\nu_{12}^k E_2^k}{1 - \nu_{12}^k \nu_{21}^k}; Q_{22}^k = \frac{E_2^k}{1 - \nu_{12}^k \nu_{21}^k}; \\ Q_{33}^k &= G_{12}^k; Q_{55}^k = G_{13}^k; Q_{44}^k = G_{23}^k \end{aligned} \quad (5)$$

In which  $E_1, E_2, G_{12}, G_{23}, G_{13}, \nu_{12}, \nu_{21}$  are independent material properties for each layer. The stress strain relationship in the global reference system  $(x, y, z)$  is given as

$$\begin{Bmatrix} \sigma_{xx}^k \\ \sigma_{yy}^k \\ \tau_{xy}^k \\ \tau_{xz}^k \\ \tau_{yz}^k \end{Bmatrix} = \begin{bmatrix} \bar{Q}_{11} & \bar{Q}_{12} & \bar{Q}_{16} & 0 & 0 \\ \bar{Q}_{12} & \bar{Q}_{22} & \bar{Q}_{26} & 0 & 0 \\ \bar{Q}_{61} & \bar{Q}_{62} & \bar{Q}_{33} & 0 & 0 \\ 0 & 0 & 0 & \bar{Q}_{55} & \bar{Q}_{54} \\ 0 & 0 & 0 & \bar{Q}_{45} & \bar{Q}_{44} \end{bmatrix}^k \begin{Bmatrix} \varepsilon_{xx}^k \\ \varepsilon_{yy}^k \\ \gamma_{xy}^k \\ \gamma_{xz}^k \\ \gamma_{yz}^k \end{Bmatrix} \quad (6)$$

where  $\bar{Q}_{ij}^k$  is the transformed material constant matrix (see [12] for more details)

From Hooke's law and the linear strains given by Eq. (2), the stress is computed by

$$\boldsymbol{\sigma} = \begin{bmatrix} \boldsymbol{\sigma}_p \\ \boldsymbol{\tau} \end{bmatrix} = \begin{bmatrix} \mathbf{D}^* & 0 \\ 0 & \mathbf{D}^s \end{bmatrix} \begin{bmatrix} \boldsymbol{\varepsilon}_p \\ \boldsymbol{\gamma} \end{bmatrix} \quad (7)$$

where  $\boldsymbol{\sigma}_p$  and  $\boldsymbol{\tau}$  are the in-plane stress component and shear stress;  $\mathbf{D}^*$  is material constant matrices given in the form as

$$\mathbf{D}^* = \begin{bmatrix} \mathbf{A} & \mathbf{B} & \mathbf{E} \\ \mathbf{B} & \mathbf{D} & \mathbf{F} \\ \mathbf{E} & \mathbf{F} & \mathbf{H} \end{bmatrix} \quad (8)$$

$$(A_{ij}, B_{ij}, D_{ij}, E_{ij}, F_{ij}, H_{ij}) = \int_{-h/2}^{h/2} (1, z, z^2, f(z), zf(z), f^2(z)) \bar{Q}_{ij} dz \quad i, j = 1, 2, 6$$

$$D_{ij}^s = \int_{-h/2}^{h/2} [(f'(z))^2] \bar{Q}_{ij} dz \quad i, j = 4, 5$$

For forced vibration analysis of the plates, weak form can be derived from the following undamped dynamic equilibrium equation,

$$\int_{\Omega} \delta \mathbf{\epsilon}_p^T \mathbf{D}^* \mathbf{\epsilon}_p d\Omega + \int_{\Omega} \delta \boldsymbol{\gamma}^T \mathbf{D}_s \boldsymbol{\gamma} d\Omega + \int_{\Omega} \delta \tilde{\mathbf{u}}^T \mathbf{m} \ddot{\mathbf{u}} d\Omega = \int_{\Omega} \delta w q(x, y, t) d\Omega \quad (10)$$

where  $q(x, y, t)$  is the transverse loading per unit area and the function depending on time and space; the mass matrix  $\mathbf{m}$  is calculated according to the consistent form given by

$$\mathbf{m} = \begin{bmatrix} I_1 & I_2 & I_4 \\ I_2 & I_3 & I_5 \\ I_4 & I_5 & I_6 \end{bmatrix}, (I_1, I_2, I_3, I_4, I_5, I_6) = \int_{-h/2}^{h/2} \rho(1, z, z^2, f(z), zf(z), f^2(z)) dz$$

in which  $\tilde{\mathbf{u}} = [\mathbf{u}_1 \quad \mathbf{u}_2 \quad \mathbf{u}_3]^T$  and

$$\mathbf{u}_1 = \begin{Bmatrix} u_0 \\ v_0 \\ w \end{Bmatrix}; \mathbf{u}_2 = \begin{Bmatrix} -w_{,x} \\ -w_{,y} \\ 0 \end{Bmatrix}; \mathbf{u}_3 = \begin{Bmatrix} \beta_x \\ \beta_y \\ 0 \end{Bmatrix}$$

where  $\rho$  is the mass density.

### III. THE LAMINATED COMPOSITE PLATE FORMULATION BASED ON NURBS BASIS FUNCTIONS

#### 1. Introduction to NURBS functions

Given a knot vector  $\Xi = \{\xi_1, \xi_2, \dots, \xi_{n+p+1}\}$ , the associated B-spline basis functions are defined recursively starting with the zero<sup>th</sup> order basis function ( $p = 0$ ) as

$$N_{i,0}(\xi) = \begin{cases} 1 & \text{if } \xi_i \leq \xi < \xi_{i+1} \\ 0 & \text{otherwise} \end{cases} \quad (13)$$

and for a polynomial order  $p \geq 1$

$$N_{i,p}(\xi) = \frac{\xi - \xi_i}{\xi_{i+p} - \xi_i} N_{i,p-1}(\xi) + \frac{\xi_{i+p+1} - \xi}{\xi_{i+p+1} - \xi_{i+1}} N_{i+1,p-1}(\xi) \quad (14)$$

A knot vector  $\Xi$  is defined as a sequence of knot value  $\xi_i \in R, i = 1, \dots, n + p$ . If the first and

the last knots are repeated  $p+1$  times, the knot vector is called open knot.

By the tensor product of basic functions in two parametric dimensions  $\xi$  and  $\eta$  with two knot vectors  $\Xi = \{\xi_1, \xi_2, \dots, \xi_{n+p+1}\}$  and

$\mathbf{H} = \{\eta_1, \eta_2, \dots, \eta_{m+q+1}\}$ , the two-dimensional B-spline basis functions are obtained as,

$N_A(\xi, \eta) = N_{i,p}(\xi) M_{j,q}(\eta)$ . Figure 2 illustrated a bivariate cubic B-spline basic function.

(11) To exactly represent some curved geometry (e.g. circles, cylinders, spheres, etc.) the non-uniform rational B-splines (NURBS) functions are used. Being different from B-spline, each control point of NURBS has additional value called an individual weight  $\zeta_A$  [8]. Thus, the NURBS functions can be expressed as  $R_A(\xi, \eta) = N_A \zeta_A / \sum_A N_A(\xi, \eta) \zeta_A$ . It can be noted that B-spline function is only the special case of the NURBS function when the individual weight of control point is constant.

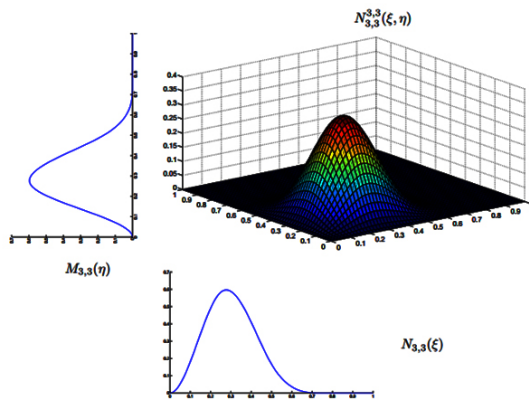


Figure 2. A bivariate cubic B-spline basis function with knot vectors.

$$\Xi = \mathbf{H} = \{0, 0, 0, 0, 0.25, 0.5, 0.75, 1, 1, 1, 1\}$$

#### 2. A higher order plate formulation based on NURBS approximation

Using the NURBS basis functions defined above, both the description of the geometry (or the physical point) and the displacement field  $\mathbf{u}$  of the plate are approximated as,

$$\mathbf{x}^h(\xi, \eta) = \sum_A^{m \times n} R_A(\xi, \eta) \mathbf{P}_A; \mathbf{u}^h(\xi, \eta) = \sum_A^{m \times n} R_A(\xi, \eta) \mathbf{q}_A \quad (15)$$

where  $n \times m$  is the number basis functions,  $\mathbf{x}^T = (x \ y)$  is the physical coordinate vector. In Eq.(15),  $R_A(\xi, \eta)$  are rational basic functions,  $\mathbf{P}_A$  are the control points and  $\mathbf{q}_A = [u_{0A} \ v_{0A} \ w_A \ \beta_{xA} \ \beta_{yA}]^T$  is the vector of nodal degrees of freedom associated with the control point A.

Substituting Eq.(15) into Eq.(3), the in-plane and shear strains can be rewritten as:

$$[\boldsymbol{\varepsilon}_p \ \boldsymbol{\gamma}]^T = \sum_{A=1}^{m \times n} [\mathbf{B}_A^m \ \mathbf{B}_A^{b1} \ \mathbf{B}_A^{b2} \ \mathbf{B}_A^s]^T \mathbf{q}_A \quad (16)$$

in which

$$\begin{aligned} \mathbf{B}_A^{b1} &= \begin{bmatrix} 0 & 0 & -R_{A,xx} & 0 & 0 \\ 0 & 0 & -R_{A,yy} & 0 & 0 \\ 0 & 0 & -2R_{A,xy} & 0 & 0 \end{bmatrix} \\ \mathbf{B}_A^{b2} &= \begin{bmatrix} 0 & 0 & 0 & R_{A,x} & 0 \\ 0 & 0 & 0 & 0 & R_{A,y} \\ 0 & 0 & 0 & R_{A,y} & R_{A,x} \end{bmatrix}, \\ \mathbf{B}_A^s &= \begin{bmatrix} 0 & 0 & 0 & R_A & 0 \\ 0 & 0 & 0 & 0 & R_A \end{bmatrix} \\ \mathbf{B}_A^m &= \begin{bmatrix} R_{A,x} & 0 & 0 & 0 & 0 \\ 0 & R_{A,y} & 0 & 0 & 0 \\ R_{A,y} & R_{A,x} & 0 & 0 & 0 \end{bmatrix} \end{aligned} \quad (17)$$

For forced vibration analysis of the plates, undamped dynamic discrete equation can be written from Eq.(10) as,

$$\mathbf{M}\ddot{\mathbf{q}} + \mathbf{K}\mathbf{q} = \mathbf{F}(t) \quad (18)$$

where the global stiffness matrix  $\mathbf{K}$  is given by

$$\mathbf{K} = \int_{\Omega} \left\{ \begin{bmatrix} \mathbf{B}_A^m \\ \mathbf{B}_A^{b1} \\ \mathbf{B}_A^{b2} \end{bmatrix}^T \begin{bmatrix} \mathbf{A} & \mathbf{B} & \mathbf{E} \\ \mathbf{B} & \mathbf{D} & \mathbf{F} \\ \mathbf{E} & \mathbf{F} & \mathbf{H} \end{bmatrix} \begin{bmatrix} \mathbf{B}_A^m \\ \mathbf{B}_A^{b1} \\ \mathbf{B}_A^{b2} \end{bmatrix} + (\mathbf{B}_A^s)^T \mathbf{D}^s \mathbf{B}_A^s \right\} d\Omega \quad (19)$$

The distributed transverse force in the  $z$  direction one has the following expression

$$\mathbf{F}(t) = \int_{\Omega} \mathbf{R}q(x, y, t) d\Omega \quad (20)$$

where

$$\mathbf{R} = [0 \ 0 \ R_A \ 0 \ 0] \quad (21)$$

The global mass matrix  $\mathbf{M}$  is expressed as

$$\mathbf{M} = \int_{\Omega} \left\{ \begin{bmatrix} \mathbf{N}_0 \\ \mathbf{N}_1 \\ \mathbf{N}_2 \end{bmatrix}^T \begin{bmatrix} I_1 & I_2 & I_4 \\ I_2 & I_3 & I_5 \\ I_4 & I_5 & I_6 \end{bmatrix} \begin{bmatrix} \mathbf{N}_0 \\ \mathbf{N}_1 \\ \mathbf{N}_2 \end{bmatrix} \right\} d\Omega \quad (22)$$

where

$$\begin{aligned} \mathbf{N}_0 &= \begin{bmatrix} R_A & 0 & 0 & 0 & 0 \\ 0 & R_A & 0 & 0 & 0 \\ 0 & 0 & R_A & 0 & 0 \end{bmatrix}; \\ \mathbf{N}_1 &= \begin{bmatrix} 0 & 0 & -R_{A,xx} & 0 & 0 \\ 0 & 0 & -R_{A,yy} & 0 & 0 \\ 0 & 0 & 0 & 0 & 0 \end{bmatrix}; \mathbf{N}_2 = \begin{bmatrix} 0 & 0 & 0 & R_A & 0 \\ 0 & 0 & 0 & 0 & R_A \\ 0 & 0 & 0 & 0 & 0 \end{bmatrix} \end{aligned} \quad (23)$$

It should be noted that for forced vibration analysis, the approximate function is done with both space and time. At time  $t + \Delta t$ , Eq.(18) should also be considered at time  $t + \Delta t$  as follows

$$\mathbf{M}\ddot{\mathbf{q}}_{t+\Delta t} + \mathbf{K}\mathbf{q}_{t+\Delta t} = \mathbf{F}_{t+\Delta t}(t) \quad (24)$$

In this paper, Eq.(18) is solved by the Newmark time integration method. This latter method assumes that the acceleration varies linearly within the interval  $(t, t + \Delta t)$

$$\begin{aligned} [\mathbf{M} + \alpha\mathbf{K}(\Delta t)^2] \ddot{\mathbf{q}}_1 &= \mathbf{F}_1 - [\mathbf{K}\mathbf{q}_0 + \mathbf{K}\Delta t\dot{\mathbf{q}}_0 + \\ &+ (\frac{1}{2} - \alpha)\mathbf{K}\ddot{\mathbf{q}}_0(\Delta t)^2] \end{aligned} \quad (26)$$

$$\dot{\mathbf{q}}_1 = \dot{\mathbf{q}}_0 + (1 - \delta)\ddot{\mathbf{q}}_0\Delta t + \delta\ddot{\mathbf{q}}_1\Delta t \quad (26)$$

$$\mathbf{q}_1 = \mathbf{q}_0 + \dot{\mathbf{q}}_0\Delta t + (\frac{1}{2} - \alpha)\ddot{\mathbf{q}}_0(\Delta t)^2 + \alpha\ddot{\mathbf{q}}_1(\Delta t)^2 \quad (27)$$

Because the Newmark time integration method is an implicit method, it will unconditionally stable if  $\delta \geq 0.5$  and  $\alpha \geq 1/4(\delta + 0.5)^2$ . Traditionally, we choose  $\alpha = 0.25$  and  $\delta = 0.5$  are used for the simplification.

#### IV. NUMERICAL EXAMPLE

In order to demonstrate the accuracy and effectiveness of the present method for transient analysis of laminated composite plates, three numerical examples with different transient loadings are studied. The obtained results are verified by comparing with other numerical or analytical solutions available in the literature or commercial software. For examples, cubic order NURBS basis function over  $11 \times 11$  elements is used. All layers of the laminated plate are assumed to have the same thicknesses and material properties. The time step  $\Delta t = 0.1 \text{ ms}$  is chosen for 4.2.1 and 4.2.2 sections.

##### 1. A three-layer square plate $[0^0/90^0/0^0]$

First, a fully simply supported three-layer square laminated plate sorted as  $[0^0/90^0/0^0]$  is considered. Material *I* is used, shown in Table 1. This example was also studied by Wang *et al.* [7] using the strip element method (SEM), which is chosen here to demonstrate the accuracy of the IGA in dynamic analysis of

plates under different transient loads including step, triangular, sine and explosive blast loads. The length and the thickness of square plates are assumed to be  $a=20h$  and  $h=0.0381 \text{ m}$ , respectively. The square plate is subjected to a transverse load which is sinusoidally distributed in spatial domain and varies with time as,

$$q(x, y, t) = q_0 \sin\left(\frac{\pi x}{a}\right) \sin\left(\frac{\pi y}{b}\right) F(t) \quad (28)$$

in which

$$F(t) = \begin{cases} \begin{cases} 1 & 0 \leq t \leq t_1 \\ 0 & t > t_1 \end{cases} & (a) \\ \begin{cases} 1-t/t_1 & 0 \leq t \leq t_1 \\ 0 & t > t_1 \end{cases} & (b) \\ \begin{cases} \sin(\pi t/t_1) & 0 \leq t \leq t_1 \\ 0 & t > t_1 \end{cases} & (c) \\ e^{-\gamma t} & (d) \end{cases} \quad (29)$$

where cases (a), (b), (c), (d) are called step, triangular, sine and explosive blast loading, respectively.

$$t_1 = 0.006 \text{ s}; \gamma = 330 \text{ s}^{-1} \text{ and } q_0 = 3.448 \text{ MPa}$$

Table 1: Properties of materials

Material	$E_1$ (GPa)	$E_2$ (GPa)	$G_{12}$ (GPa)	$G_{13}$ (GPa)	$G_{23}$ (GPa)	$\nu_{12}$	$\rho$ (kg / m <sup>3</sup> )
I	172.369	6.895	3.448	3.448	3.448	0.25	1603.03
II	172.369	6.895	3.448	3.448	1.379	0.25	1603.03
III	131.69	8.55	6.67	6.67	6.67	0.3	1610

Figure 3 shows the time histories of central deflection of the plate under various dynamic loadings. The obtained results of present solution using IGA are compared with those obtained by Wang *et al.* [7] using the strip element method (SEM). As expected, the effectiveness of this work is fully believable when profiles relatively coincide with Wang's solutions.

Second, a fully simply supported three-layer square laminated plate sorted as  $[0^0/90^0/0^0]$  is also considered. Material *II* is used. The length and thickness of the plates are assumed to be  $a = 5h$  and  $h = 0.1524 \text{ m}$ , respectively. As above example, the plate is

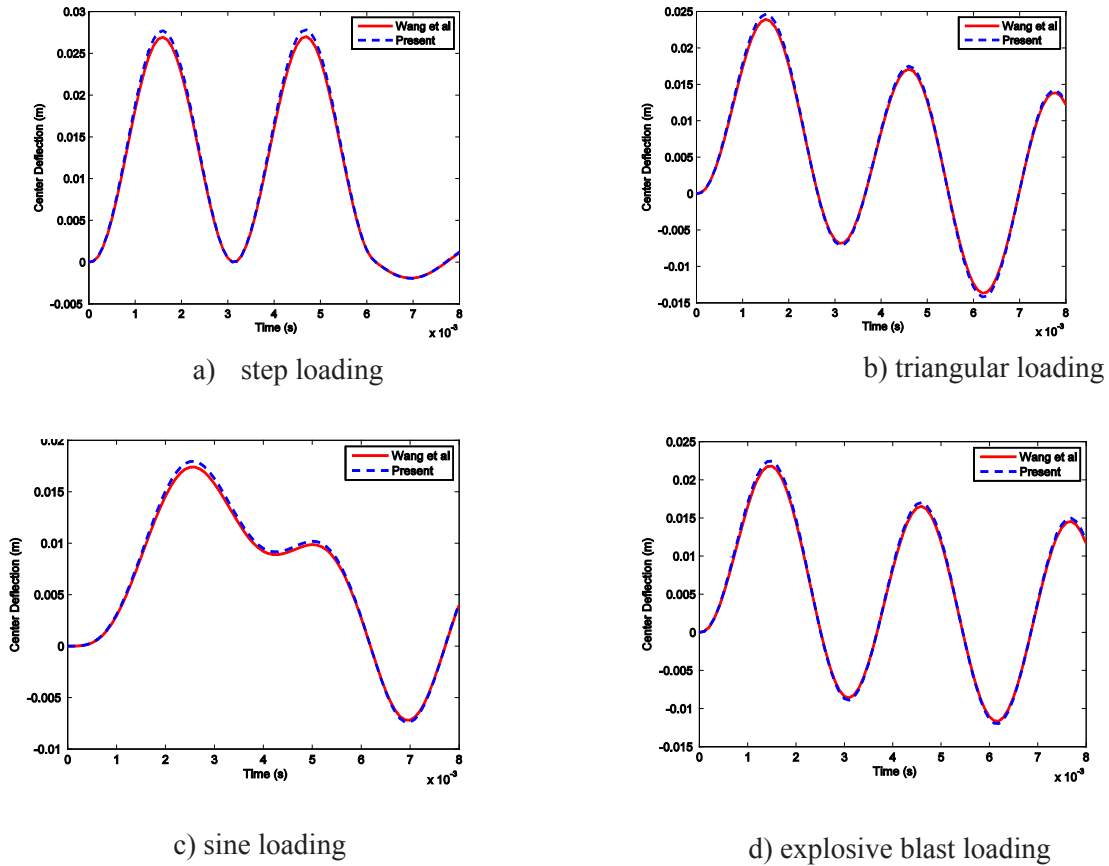


Figure 3. Variation of the center deflection as a function of time for a (00/900/00) square laminated composite plate subjected to various dynamic loadings.

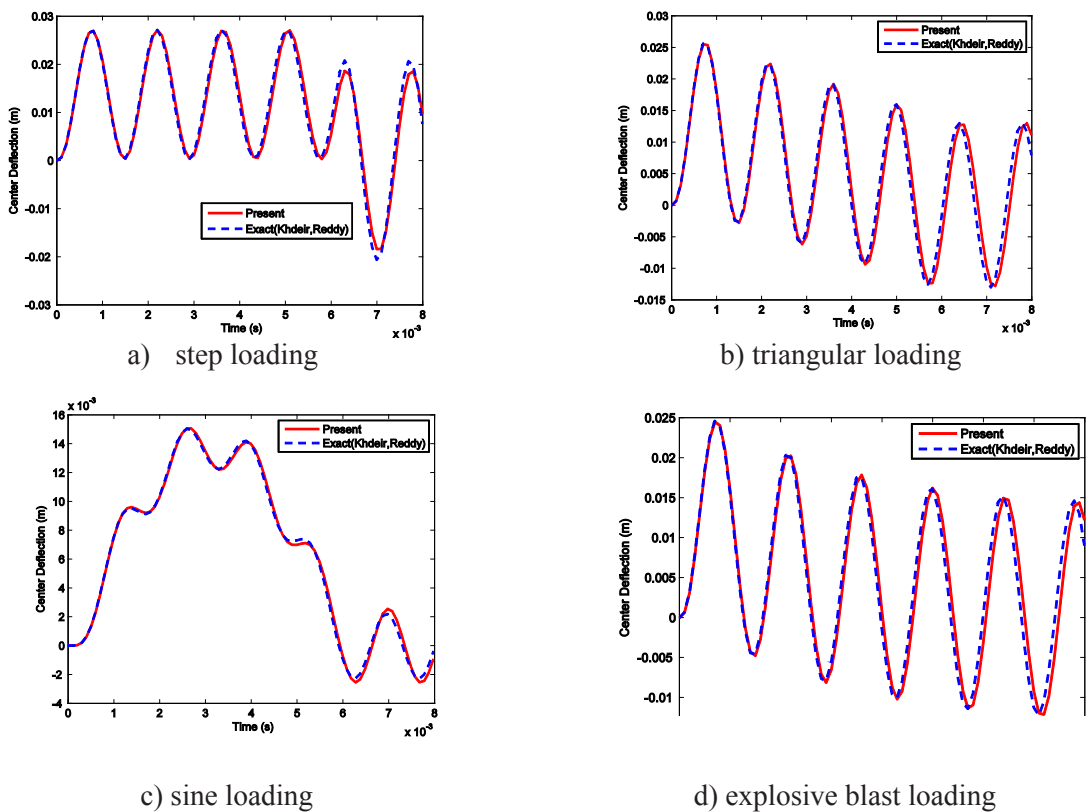


Figure 4. Central deflection versus time for a  $[0^0/90^0/0^0]$  square laminated plate subjected to various dynamic loadings.

also subjected to sinusoidal a distributed transverse load (with  $q_0 = 68.9476$  MPa ). The displacement at the center of plate is also studied. This benchmark solution was originally investigated by Khdeir and Reddy [13]. Figure 4 shows variation of the displacement at the center of plate as a function under various dynamic loadings. The present solutions based on IGA and TSdT are compared with exact solution of Khdeir and Reddy [13] based on HSdT. As observed in Figure 4, the profiles are relatively exact and errors are very small and approvable when comparing with exact solution.

## 2. A four- layer square plate [30°/-30°/-30°/30°]

Let us consider a four-layer angle-ply square laminated plate arranged as [30°/-30°/-30°/30°]. Material III is used. The length to thickness ratio of the plate is assumed to be  $a/h = 50$ . The plate is too subjected to a transverse load which is uniformly distributed as, called conventional blast loading [7].

$$q(x, y, t) = q_0 \left(1 - \frac{t}{t_2}\right) e^{-\alpha_1 t / t_2} \quad (30)$$

in which  $q_0 = 68.9476$  KPa  $t_2 = 0.004s$   $\alpha_1 = 1.98$   
 The time history of the deflection at the center of the four-layer fully clamped (CCCC) laminated plate is investigated, as shown in Figure 5. The results are compared with Wang's solutions [7]. From Figure 5, the present results match well with Wang's results.

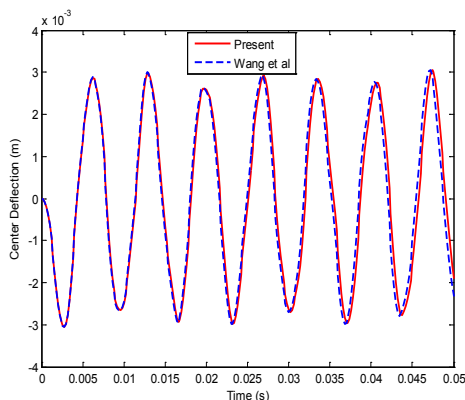


**Figure 5.** The time history of the center deflection of the [30°/-30°/-30°/30°] fully clamped laminated plate.

## 3. A circular four-layer plate [45°/-45°/-45°/45°]

Finally, to increase lively for numerical examples and obtain the desired effect, we consider a [45°/-45°/-45°/45°] circular plate with fully clamped (CCCC) boundary condition as shown Figure 6a. Material parameter III is also used. The plate is subjected to a conventional blast load as

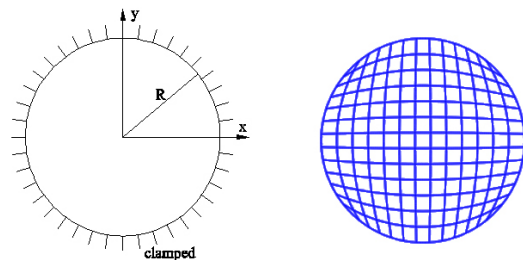


**Figure 6.** The circular plate: (a) geometry and (b) mesh based on 13x13 cubic elements.

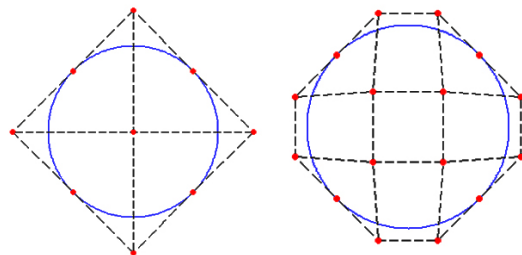


**Figure 7.** Coarse mesh and control points of a circular plate with various degrees: a)  $p=2$  and b)  $p=3$ .

given in Section 4.2.2. The circular plate has a radius to thickness ratio is 10 ( $R/h = 10$ ). A rational quadratic basis is enough to model exactly the circular geometry. Coarse mesh and control net of the plate with respect to quadratic and cubic elements are illustrated in Figure 7. Time step is chosen  $\Delta t = 0.4ms$ . The plate is meshed with 13x13 NURBS cubic elements as shown Figure 6b. Figure 8 illustrates the profile of displacements versus time at the center of the circular plate subjected to conventional blast load. Obtained results are compared with solution from ANSYS 13 which using SHELL 181 elements. It can be seen that the present solutions are in good agreement with the solution from ANSYS software.

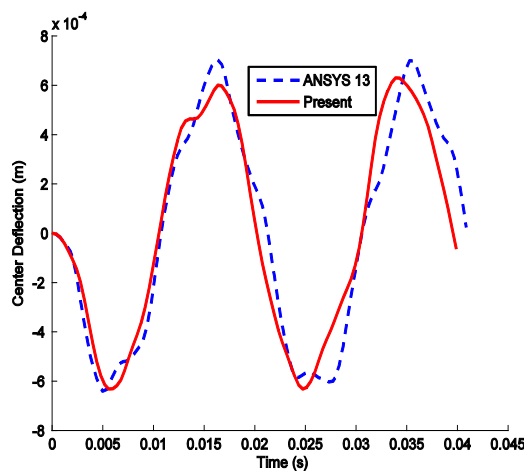


Figure 8. The deflection at the center of the  $[45^{\circ}/-45^{\circ}/-45^{\circ}/45^{\circ}]$  circular laminated plate subjected to a conventional blast load.

## V. CONCLUSIONS

Isogeometric analysis combined with TSDT to analyze the transient of laminated composite plates is first studied. The Newmark time-integration algorithm was chosen to approximate the ordinary differential equations in time. We have successfully presented an application of the NURBS-based isogeometric finite element approach to transient analysis for laminated composite plates as this work. The IGA have expressed well its role in solving the practical problems with saving in cost, high accuracy. The numerical results agree well with those of available references and exact solution, and hence illustrated the accuracy and effectiveness of the present method.

## REFERENCES

- [1] H. Reismann, Forced motion of elastic plates, *Journal of Applied Mechanics* 35, pp.510-515, 1968.
- [2] H. Reismann, Y. Lee, Forced motion of rectangular plates, *Development in Theoretical and Applied Mechanics*, 4, pp.3-18,1969.
- [3] T. Rock, E. Hinton, Free vibration and transient response of thick and thin plates using the finite element method, *Earthquake Engineering and Structural Dynamics*, 3, pp.51-63, 1974.
- [4] H.U. Akay, Dynamic larger deflection analysis of plates using mixed finite elements, *Computers and Structures*, 11, pp.1-11,1980.
- [5] J.N. Reddy, Dynamic (transient) analysis of layered anisotropic composite-material plates, *International Journal for Numerical Methods in Engineering*, 19, pp.237-255,1983.
- [6] Mallikarjuna, T. Kant, Dynamics of laminated composite plates with a higher order theory and finite element discretization, *Journal of Sound and Vibration*, 126, pp.463-475,1988.
- [7] Y.Y. Wang, K.Y. Lam, G.R. Liu, A strip element method for the transient analysis of symmetric laminated plates, *International Journal of Solids and Structures*, 38, pp.241-259,2001.
- [8] T.J.R. Hughes, J.A. Cottrell, Y. Bazilevs, Isogeometric analysis: CAD, finite elements, NURBS, exact geometry and mesh refinement, *Computer Methods in Applied Mechanics and Engineering*, 194, pp.4135-4195, 2005.
- [9] Chien. H. Thai, A.J.M. Ferreira, T. Rabczuk, S.P.A Bordas, H. Nguyen-Xuan, Isogeometric analysis of laminated composite and sandwich plates using a new inverse trigonometric shear deformation theory, *European Journal of Mechanics - A/Solids*, 43, pp.89-108, 2014.
- [10] N.Valizadeh, S.S. Ghorashi, H. Yousefi, T.Q. Bui, T.Rabczuk, Transient Analysis of Laminated Composite Plates using Isogeometric Analysis, *the Eighth International Conference on Engineering Computational Technology; Civil-Comp Press, Stirlingshire, Scotland*, 2012.

- [11] J.N. Reddy, A simple higher-order theory for laminated composite plates, *Journal of Applied Mechanics*, 51, pp.745 – 752,1984.
- [12] J.N. Reddy, *Mechanics of Laminated Composite Plates and Shells Theory and Analysis, second ed.* CRC Press, New York, 2004.
- [13] A.A. Khdeir, J.N. Reddy, Exact solution for the transient response of symmetric cross-ply laminates using a higher-order plate theory, *Composite Science and Technology*, 34, pp.205-224, 1989.